Am J Transl Res 2020;12(7):3984-3992
www.ajtr.org /ISSN:1943-8141/AJTR0110618

Original Article

Quantitative analyses of the correlation between dynamic contrast-enhanced MRI and intravoxel incoherent motion DWI in thyroid nodules

Minghui Song[1*], Yunlong Yue[1*], Jinsong Guo[1], Lili Zuo[1], Hong Peng[2], Queenie Chan[3], Yanfang Jin[1]

Departments of [1]MR, [2]Otolaryngology, Beijing Shijitan Hospital, Capital Medical University, Peking University Ninth School of Clinical Medicine, Beijing, China; [3]Philips Healthcare, Shatin, New Territories, Hong Kong, China. [*]Equal contributors.

Received March 10, 2020; Accepted June 26, 2020; Epub July 15, 2020; Published July 30, 2020

Abstract: This study investigated the correlation between dynamic contrast-enhanced magnetic resonance imaging (DCE-MRI) and intravoxel incoherent motion diffusion-weighted imaging (IVIM DWI) to differentiate thyroid nodules. Quantitative DCE-MRI parameters, including the transfer constant (K^{trans}), rate constant (K_{ep}) and volume fraction of the extracellular extravascular space (V_e), were calculated. The diffusion coefficient (*D*), pseudo-diffusion coefficient (D^*), and perfusion fraction (*f*) were derived from biexponential fitting of IVIM DWI. A total of 38 nodules, including 22 malignant and 16 benign nodules, were analyzed. The K^{trans}, K_{ep} and V_e for benign lesions were 1.32 ± 0.76 min^{-1}, 6.44 ± 1.44 min^{-1}, and 2.02 ± 0.89 min^{-1}, respectively, and for malignant lesions, the values were 0.84 ± 0.30 min^{-1}, 5.43 ± 1.38 min^{-1}, and 1.71 ± 0.83 min^{-1}, respectively (*P* = 0.027, 0.036, and 0.257, respectively). The *D*, *f*, and D^* for benign lesions were 1.51 ± 0.52 mm^2/s, 26.63 ± 8.75%, and 15.84 ± 8.71 mm^2/s, respectively, and for malignant lesions, the values were 0.68 ± 0.17 mm^2/s, 31.63 ± 10.72%, and 11.10 ± 4.21 mm^2/s, respectively (*P* [< 0.0001, 0.135, 0.058], respectively). No significant correlations were found between IVIM DWI and DCE-MRI quantitative parameters (all $P > 0.05$). In benign nodules, a moderate inverse correlation was found between *D* and K_{ep} ($r = -0.54$, $P = 0.031$). IVIM DWI shows no significant correlation with perfusion parameters derived from DCE-MRI; however, IVIM DWI combined with quantitative DCE-MRI may be a useful imaging tool for the assessment of thyroid nodules in clinical studies.

Keywords: Contrast media, diffusion weighted magnetic resonance imaging, thyroid nodule

Introduction

Thyroid cancer is the most common malignant disease of the endocrine system. Although most papillary carcinomas exhibit poor invasiveness, some malignant nodules with abundant blood supply have obvious distant metastasis and a poor prognosis [1]. Early imaging approaches include ultrasound, computed tomography (CT) and conventional diffusion-weighted imaging (DWI). These methods are typically used to observe the morphology of thyroid nodules, but they cannot be quantified and compared with each other. In recent years, diffusion-weighted functional imaging has been gradually applied for the diagnosis of thyroid disease. Many research foused on the diagnositic value of quantitative dynamic contrast-enhanced magnetic resonance imaging (DCE-MRI) and intravoxel incoherent motion (IVIM) DWI.

DCE-MRI parameters are likely attributed to their direct reflection of tissue physiology based on the concentration of contrast agent and are more closely linked to perfusion and permeability; thus, they are related to tumor angiogenesis [2, 3]. The application of DCE-MRI in differentiating thyroid nodules has been investigated for more than twenty years. Due to limitations in hardware and software applications and the heterogeneity of thyroid nodules, initial studies focused on the time-intensity curve. The semiquantitative parameters in these studies yielded different results upon applying semiquantitative DCE-MRI in benign and malignant thyroid

nodules [4-7]. Quantitative DCE-MRI, a pharmacokinetic model, was originally proposed by Tofts et al. [8] to quantitatively determine capillary blood flow in tumors. These parameters can describe complex microcirculation in living tissues and provide quantitative information about vascular permeability and angiogenesis. However, quantitative DCE-MRI analysis using a 1.5T scanner in differentiate benign and malignant thyroid nodules need further exploration [9]. Nevertheless, with improvements in MRI hardware and image acquisition technology, image quality and time resolution have significantly improved. This study analyzed the dynamic contrast enhancement of benign and malignant thyroid nodules using a 3.0T scanner. DCE-MRI requires contrast agents to provide perfusion information, which may limit its application in patients who cannot receive contrast agents. IVIM DWI has shown great potential for reflecting the diffusivity and microvascular perfusion of tissues without the use of contrast agents [10]. In early studies of thyroid nodules, IVIM DWI successfully showed its feasibility for differentiating benign and malignant nodules [11, 12]. Furthermore, several studies have demonstrated correlations between parameters from IVIM DWI and DCE-MRI in the head and neck, mainly in the nasopharynx and nasal sinus and in parotid gland tumors and metastatic lymph nodes [13-15]. However, Xu et al. [16] suggested that IVIM DWI cannot replace DCE-MRI for benign and malignant tumors of the head and neck, especially squamous cell carcinoma. Conversely, no related reports on thyroid nodules have been published.

The aim of this study was to assess the correlations of IVIM DWI parameters with quantitative DCE-MRI parameters and evaluate their diagnostic performance.

Materials and methods

Patient population

This study was approved by the local ethics committee in our institution, and written informed consent was obtained. Patients meeting the following inclusion criteria were included in this study: 1) thyroid nodules or masses detected by physical examination or incidentally; 2) thyroid nodules larger than 1.5 cm detected by ultrasonography; and 3) a belief of clinicians and/or patients that the lesion should be removed surgically. For some nodules that were suspected to be benign, surgical treatment was planned according to the patient's preferences or symptoms. The exclusion criteria were as follows: 1) pure cysts/necrotic nodules; 2) the presence of any MRI-incompatible metallic device; or 3) motion artifacts during MRI exams.

Between November 2017 and April 2019, 36 patients (5 men, 31 women; mean age, 54 ± 11 years; age range, 21-69 years) with 38 thyroid nodules were recruited. The pathological findings confirmed 16 benign nodules and 22 malignant nodules with the following diagnoses: papillary thyroid cancer (n = 21), medullary thyroid carcinoma (n = 1), nodular goiter (n = 14) and thyroid adenoma (n = 2). Thirty-four patients had solitary thyroid nodules, and 2 patients had two nodules.

MRI protocol

All patients underwent preoperative MRI exams (Philips 3.0T Ingenia, Philips Medical System, the Netherlands). Before performing DCE-MRI, routine T1-weighted imaging (T1WI), T2-weighted imaging (T2WI) and IVIM DWI data were acquired using an 8-channel phased-array carotid coil. First, T1/T2-weighted turbo spin-echo sequences were used to capture morphologic features of the thyroid nodules. The imaging parameters for T1WI/T2WI were as follows: repetition time (TR): 525/3600 ms; echo-time (TE): 36/100 ms; field of view (FOV): 22 × 22 × 29 cm; in-plane resolution: 0.85 × 0.85 mm/0.76 × 0.76 mm; number of slices: 20; slice thickness: 4 mm; slice spacing: 0.6 mm; turbo factor: 8/22; and total acquisition time: 6:34 min. Second, iZOOM DWI was performed using a 2D RF pulse with the following parameters: TR/TE: 1351/69 ms; turbo factor, 29; echo-planar imaging factor: 29; FOV: 160 × 47 mm; acquisition matrix: 106 × 144; number of averages: 4; number of slices: 10; slice thickness: 5 mm and slice spacing: 1 mm. Eight b-values (0, 20, 50, 100, 200, 400, 600, and 990 s/mm^2) were used, and the acquisition time was 5:37 min. DCE-MRI involved a 3D fast field echo with two flip angles (5° and 15°) to determine the T1 relaxation time of the tissue before contrast agent injection (TR/TE: 3.3/1.6 ms; FOV: 220 × 220 mm; acquisition matrix: 184 × 158; reconstruction matrix: 224 × 224, number of

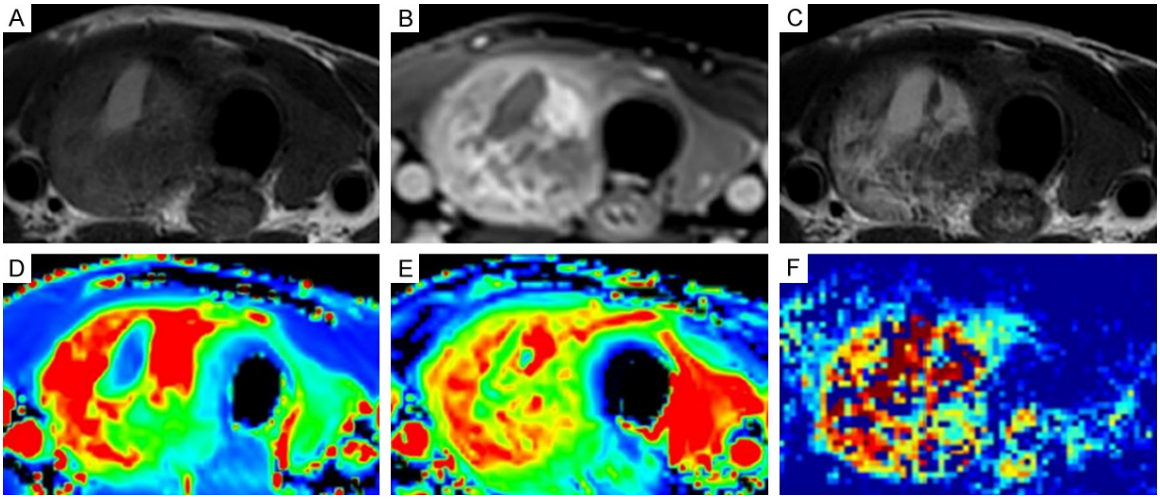

Figure 1. MRI Images of a 48-year-old man with a nodular goiter in the right lobe. Pre-contrast T1-weighted MRI (A), contrast-enhanced MRI (B) and T2-weighted MRI (C) showing a mass in the right palatine tonsil. Color coded: K^{trans} (D), K_{ep} (E), and D (F) maps derived from DCE-MRI and IVIM DWI. K^{trans} = 2.41 min^{-1}, K_{ep} = 7.80 min^{-1}, and D = 1.21 × 10^{-3} mm^2/s.

slices: 9; slice thickness: 8 mm, and slice spacing: 4 mm). By setting the flip angle to 10°, we were able to keep the remaining scanning parameters consistent with those described above. Thirty-five dynamics were acquired consecutively, with a temporal resolution of 4.3 s, and the acquisition time was 4:36 min. At the fourth dynamic, 0.1 mmol/kg of gadopentetate dimeglumine contrast agent was administered intravenously at a rate of 2.5 ml/s, followed by 20 ml of 0.9% saline flush.

Image analysis

Region of interest placement: First, a T2W MRI slice showing the largest range of solid signals was selected. Second, the region with the most obvious enhancement was selected from the dynamic enhancement sequence for delineation of the regions by avoiding necrotic tissues and vascular regions as much as possible. Third, oval regions of interest (ROIs) ranging from 20 to 50 mm^2 in size were placed on DCE and IVIM DW MRI images while every effort was taken to ensure that the ROIs were located at the same place and had the same shape (**Figures 1** and **2**). The positions of the ROIs were verified by a head and neck radiologist (S.M.H., with 10 years of post-fellowship experience in reading MRI data). Each lesion was measured twice, and the measurements were averaged.

Quantitative measurements: DCE-MRI processing was performed using commercial software (ISP Permeability; Philips Healthcare, Best, the Netherlands) that utilizes a commonly used 2-compartment pharmacokinetic model proposed by Tofts et al. [8]. T1 map images were generated using a dual-flip angle method and registered to the motion-corrected images. The two-compartment model and perfusion parameters were calculated as follows: $dC_t(t)/dt = K^{trans}C_p(t)-K_{ep}C_t(t)$, where $C_t(t)$ is the gadolinium concentration in the tumor, $C_p(t)$ is the concentration in the arterial plasma, K^{trans} is a rate constant representing the transfer of contrast agent from arterial blood to the extravascular extracellular space (EES), K_{ep} is a rate constant representing the transfer of contrast agent from the EES to blood plasma, and $V_e = K^{trans}/K_{ep}$ is the EES volume of distribution.

IVIM DWI processing was conducted using MATLAB (Mathworks, Natick, MA, R2012b). Nonlinear fitting of the biexponential model was performed as described by Le Bihan et al. [10]. The IVIM DW images were also subjected to autocorrection, and the IVIM DWI model was mathematically expressed as follows: $S_b/S_0 = (1-f) \times e^{-bD} + f \times e^{-b(D+D^*)}$, where S_b and S_0 are the signal intensities in the diffusion gradient factors of b and 0, respectively, f is the fractional volume of capillary blood, D is the diffusion coefficient, and D^* is the perfusion-related diffusion coefficient.

Statistical analysis

Statistical analysis was performed using MedCalc Online (v17.7.2). Continuous variables wi-

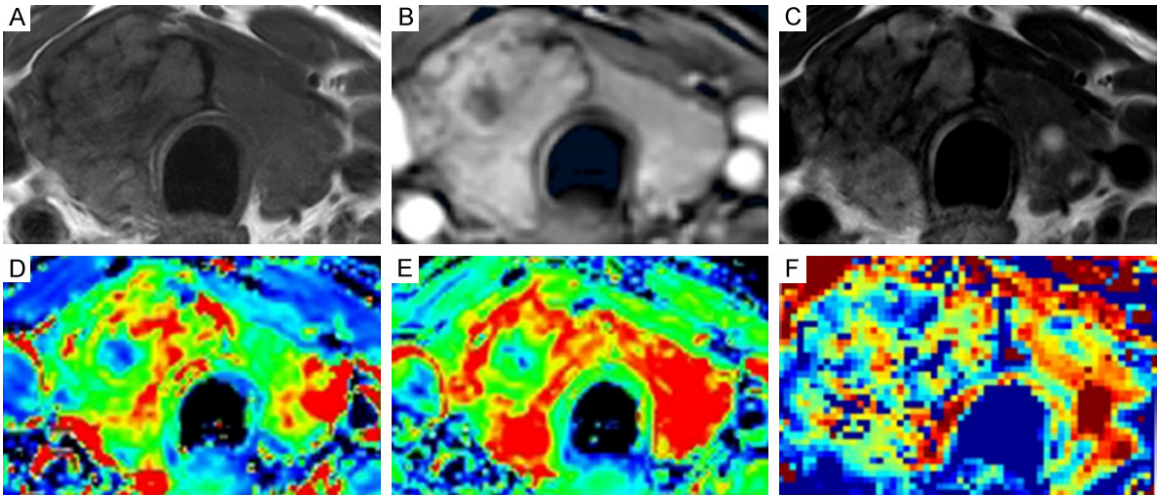

Figure 2. MRI images of a 62-year-old man with right lobe papillary thyroid cancer. Pre-contrast T1-weighted MRI (A), contrast-enhanced MRI (B) and T2-weighted MRI (C) showing a mass in the right palatine tonsil. Color coded: K^{trans} (D), K_{ep} (E), and D (F) maps derived from DCE-MRI and IVIM DWI. K^{trans} = 1.19 min^{-1}, K_{ep} = 5.40 min^{-1}, and D = 0.59 × 10^{-3} mm^2/s.

th a normal distribution are expressed as the mean ± standard deviation. The mean values of the parameters of the malignant group and the benign group were compared using independent-sample T-tests. Receiver operating characteristic (ROC) curve analysis was used to determine the optimal cut-off values of the significant parameters. The area under the ROC curve (AUC), sensitivity, specificity, positive predictive value (PPV), negative predictive value (NPV) and accuracy were computed. Multivariate logistic regression analysis was used to assess the diagnostic effects of DCE-MRI and IVIM DWI models, gauge their independent predictive value, and determine which combination of models (parameters with a significant difference in distinguishing benign and malignant thyroid nodules) was the most predictive of thyroid nodules. Pearson's correlation coefficients were computed to characterize associations between DCE-MRI and IVIM DWI parameters. A correlation coefficient $|r| < 0.5$ was considered a poor correlation, an $|r|$ value between 0.5 and 0.8 was considered a moderate correlation, and $|r| > 0.8$ was accepted as a strong correlation. $P < 0.05$ indicated a statistically significant difference.

Results

Quantitative DCE-MRI and IVIM DWI parameters

The largest diameters of the lesions ranged from 15 mm to 89 mm, with a mean of 38.8 mm. In the benign group, the values of the DCE-MRI parameters were as follows: K^{trans}: 1.32 ± 0.76 min^{-1}, K_{ep}: 6.44 ± 1.44 min^{-1}, and V_e: 2.02 ± 0.89 min^{-1}. In the malignant group, the values of the DCE-MRI parameters were as follows: K^{trans}: 0.84 ± 0.30 min^{-1}, K_{ep}: 5.43 ± 1.38 min^{-1}, and V_e: 1.71 ± 0.83 min^{-1}. Among the three DCE-MRI parameters, the K^{trans} and K_{ep} values were significantly lower in malignant nodules than in benign nodules (P = 0.027 and 0.036, respectively), while the V_e value showed no significant difference between malignant and benign nodules (P = 0.257).

In the benign group, the values of the IVIM DWI parameters were as follows: D: 1.51 ± 0.52 × 10^{-3} mm^2/s, f: 26.63 ± 8.75%, and D^*: 15.84 ± 8.71 × 10^{-3} mm^2/s. In the malignant group, the values of the IVIM DWI parameters were as follows: D: 0.68 ± 0.17 × 10^{-3} mm^2/s, f: 31.63 ± 10.72%, and D^*: 11.10 ± 4.21 × 10^{-3} mm^2/s. Among the three IVIM DWI parameters, the D value was significantly lower in malignant nodules than in benign nodules ($P < 0.0001$), while the f and D^* values showed no significant differences between malignant and benign nodules (P = 0.135 and P = 0.058, respectively).

The respective optimal cut-off values obtained from ROC curve analyses (i.e., the sensitivity, specificity, PPV, NPV and accuracy) were as follows: K^{trans}: 1.36 min^{-1} (100%, 50%, 73.33%, 100%, and 78.95%, respectively); K_{ep}: 7.39 min^{-1} (63.64%, 81.25%, 84.21%, 68.42%, and

Table 1. Comparisons of parameters from DCE-MRI and IVIM DWI between benign and malignant thyroid nodules

	K^{trans} (min^{-1})	K_{ep} (min^{-1})	K^{trans} + K_{ep}	D (× 10^{-3} mm^2/s)	D + K^{trans} + K_{ep}
AUC (95% CI)	0.668 (0.496-0.812)	0.682 (0.538-0.843)	0.719 (0.550-0.852)	0.969 (0.854-0.999)	0.991 (0.892-1.000)
Cut-off value	1.36	5.60	0.56	0.81	0.69
Sensitivity	100%	63.64%	81.82%	81.82%	90.91%
Specificity	50%	81.25%	62.50%	100%	100%
PPV	73.33%	84.21%	66.67%	100%	100%
NPV	100%	68.42%	63.64%	80%	88.89%
Accuracy	78.95%	76.32%	65.79%	89.47%	94.74%

Note: AUC, Area under the receiver operating curve; CI, Confidence intrerval; PPV, Positive predictive value; PPV, Positive predictive value.

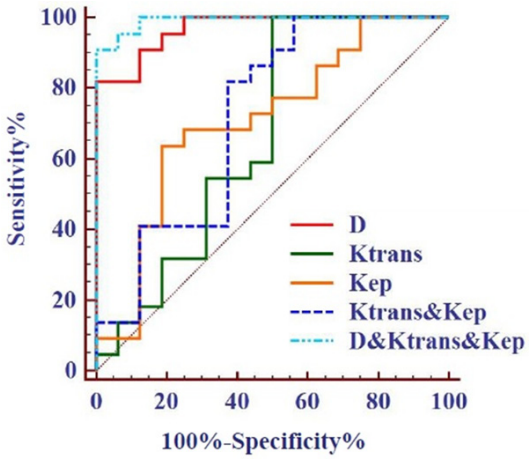

Figure 3. ROC curve analysis of the combination of DCE-MRI parameters, IVIM parameters, K^{trans}, K_{ep} and D. Regarding independent parameters, D achieved the highest AUC (0.969). The AUC of the DCE-MRI model combined with the D value was 0.991, which did not significantly differ from that of D (P = 0.224).

76.32%, respectively); and D: 0.81 × 10^{-3} mm^2/s (81.82%, 100%, 100%, 80%, and 89.47%, respectively) (summarized in **Table 1**). Respective ROC curves and AUC values are presented in **Table 1** and **Figure 3**. Regarding independent parameters, D achieved the highest AUC (0.969; 95% CI: [0.854-0.999]) in differentiating malignant from benign thyroid nodules. The DCE-MRI model constructed by multivariate logistic regression analysis yielded the following results: AUC: 0.719, sensitivity: 81.82% and specificity: 62.50%. The DCE-MRI model combined with the D value constructed by multivariate logistic regression analysis yieled the following results: AUC: 0.991, sensitivity: 90.91% and specificity: 100%, which did not significantly differ from those of D (P = 0.224).

Relationship between IVIM DWI and DCE-MRI parameters

In thyroid nodules, no significant correlations were found between IVIM DWI and DCE-MRI quantitative parameters (**Table 2**).

The stratified analysis showed that in benign nodules, a significant inverse but moderate correlation existed between D and K_{ep} (r = -0.54, P = 0.031), and no significant correlation was found between D and K^{trans} (r = -0.09, P = 0.754). In malignant nodules, no significant correlation was found between D and K^{trans} (r = -0.42, P = 0.050) or between D and K_{ep} (r = 0.10, P = 0.650) (**Figure 4**).

Discussion

In this study, both DCE-MRI parameters (K^{trans} and K_{ep}) and the IVIM DWI parameter (D) were able to significantly differentiate malignant and benign thyroid nodules. K^{trans} and K_{ep} combined with D achieved the greatest AUC value. The D value demonstrated a strong correlation with the K_{ep} value in the benign group.

The quantitative parameters of DCE-MRI (K^{trans} and K_{ep}) have been described in many studies as potentially powerful tools that can be used to assess lesion perfusion and may increase with increasing microvascular blood flow, vascular permeability, and microvessel density of the diseased tissue. The quantitative parameters of malignant lesions in the head and neck [15, 16], breast [17] and rectum [18] have been found to be significantly higher than those in benign lesions, which might suggest that a high K^{trans} and K_{ep} may reflect increased microvascular and endothelial permeability. Theoretically, permeability in the malignant nodule

Table 2. Correlation coefficients (*P* Values) between perfusion parameters derived from DCE-MRI measurements and IVIM DWI parameters

	D	*f*	*D**
K^{trans}	0.16 (*P* = 0.328)	0.17 (*P* = 0.317)	-0.03 (*P* = 0.830)
K_{ep}	-0.05 (*P* = 0.785)	0.10 (*P* = 0.545)	-0.23 (*P* = 0.159)
V_e	0.14 (*P* = 0.392)	0.20 (*P* = 0.219)	0.04 (*P* = 0.800)

group is assumed to be higher than that in the benign nodule group. Some inconsistencies have emerged between ultrasound and pathology findings in microvessel density studies of benign and malignant thyroid nodules. One pathological study showed that the microvessels of thyroid cancer were more numerous [19]. However, some ultrasound imaging studies have found that the parameters related to microvessels in malignant nodules are significantly lower than those in benign nodules [20, 21]. K^{trans} and K_{ep} were significantly lower in the malignant group than in the benign group in this study, which is consistent with the above-mentioned ultrasound study and with a previous DCE-MRI study in thyroid nodules [9]. The main reasons are as follows: 1) most of the malignant nodules were papillary carcinoma, and no further stratification was performed; 2) although many microvessels are present in malignant thyroid nodules, we speculate that most may be dysplastic microvessels, and permeability measurement represents a type of functional microvessel density; and 3) the application of a quantitative permeability model to calculate thyroid nodules and selection of the arterial input function (AIF) still require further discussion. This model is based on a well-described two-compartment model, and the thyroid is an endocrine organ with an abundant blood supply. Because the results of manually drawing the AIF in the preliminary experiment were not stable, this study used a universal AIF derived mainly from healthy subjects and based on the head and neck research basis that the AIF has very similar profiles in similar subjects [22]. Notably, a previous quantitative study failed to distinguish benign from malignant thyroid nodules [9], which we speculate may be related to the data and sample size deviations caused by the heterogeneity of lesions and the high variability of the patients. The analysis selected the largest areas of the thyroid nodules, including cystic necrosis and calcification areas, to delineate the ROIs, which might increase interference from heterogeneous factors in lesions. The purpose of this study was to explore whether IVIM DWI parameters were correlated with DCE-MRI quantitative parameters. Patients with thyroid nodule diameters greater than 1.5 cm were enrolled in the study, and necrotic lesions were avoided. We found that measurements of quantitative DCE-MRI parameters for lesions with diameters less than 1 cm were unstable. Based on the experimental design described above, the quantitative DCE-MRI parameters obtained in this study have significant differences. Our sensitivity and specificity measures were based on thresholds derived from our population and therefore likely represent overestimations of potential findings in other populations. This study found no significant difference in V_e values between benign and malignant thyroid nodules. V_e reflects the volume of contrast agent outside the EES, which is highly unstable.

No significant differences in the *f* and *D** values related to IVIM perfusion were identified. As a diffusion-related parameter, the *D* value could effectively differentiate between benign and malignant thyroid nodules, as reported in other studies [11, 23]. We speculate that the reason for the above results is related to the structure of the thyroid gland and the pathological characteristics of malignant lesions. Approximately 90% of thyroid cancers are papillary carcinomas originating from the follicular epithelium. Current studies on DWI mostly suggest that the diffusion-limited signal of malignant nodules is caused by a change in normal acinar components [9, 24, 25]. However, other studies have shown that the *f* value has statistical significance in differentiating benign and malignant thyroid nodules [12]. Because of the heterogeneity of thyroid nodules and the complexity of head and neck DWI technology, different scanning parameters, ROI delineations and enrolled patients may lead to inconsistent data.

In theory, the transport of tracers to tissues depends on the intravascular flow; therefore, the exact relationships between IVIM DWI parameters and DCE-MRI parameters may prove to be close [26]. Our results showed no significant correlations between IVIM DWI and DCE-MRI quantitative parameters in thyroid nodules, even in the malignant nodule group. Notab-

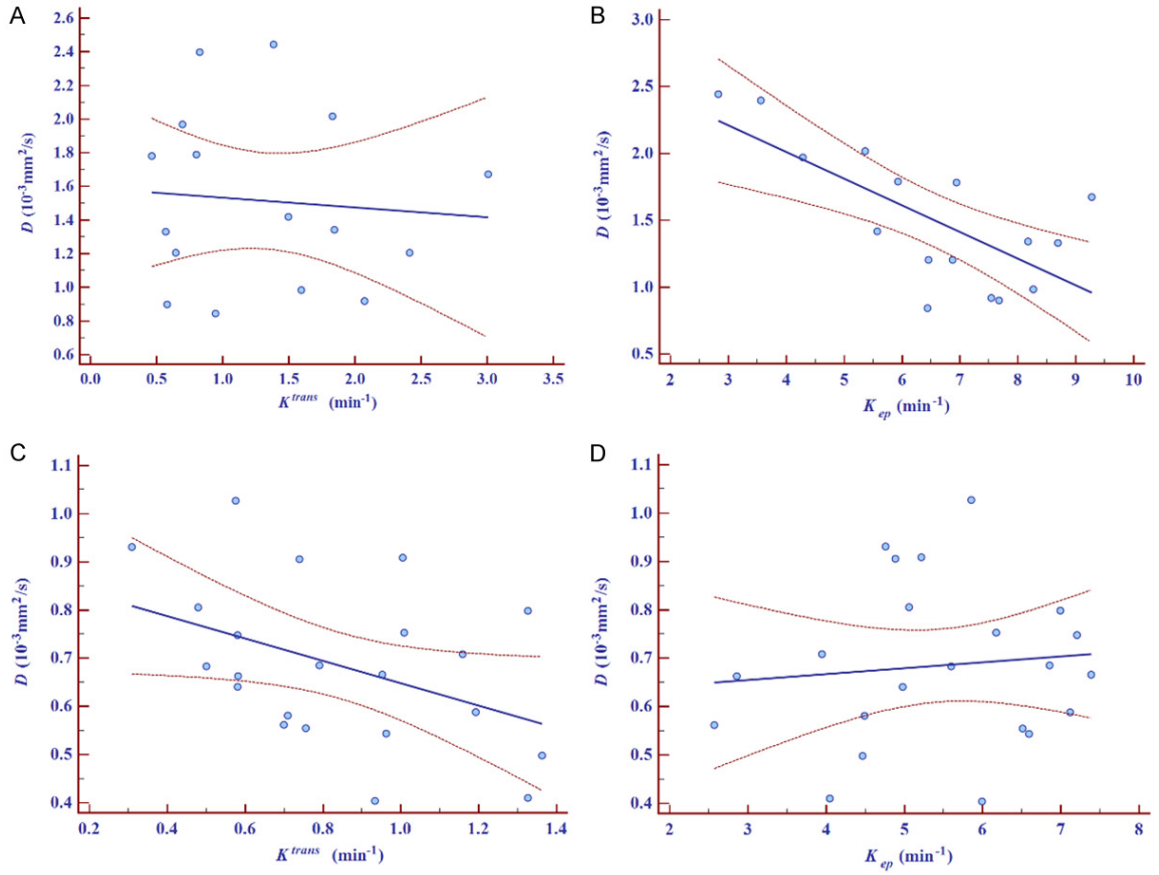

Figure 4. Pearson's correlation between DCE-MRI perfusion parameters (K^{trans}, K_{ep}) and the IVIM DWI perfusion parameter (D). In benign nodules, no significant correlation was found between D and K^{trans} (r = -0.09, P = 0.754) (A), and a significant inverse but moderate correlation was found between D and K_{ep} (r = -0.54, P = 0.031) (B). In malignant nodules, no significant correlation was found between D and K^{trans} (r = -0.42, P = 0.050) (C) or between D and K_{ep} (r = 0.10, P = 0.650) (D).

ly, the IVIM DWI and DCE-MRI parameters in this study did not clearly show the characteristic of high perfusion in malignant thyroid nodules. The poor correlations between the two methods may be explained by the above phenomena. Another explanation for the poor correlations is that the quantitative parameters of DWI and DCE-MRI are used to evaluate the different contents of tumor tissues, the former of which is mainly affected by changes in cell density in tumor tissues, while the latter is mostly affected by changes in blood perfusion and capillary permeability in tumor tissues. DCE-MRI quantitative parameters change earlier than those of DWI. Further stratification confirmed that the D value (a robust parameter) was significantly and moderately correlated with K_{ep} (a more accurate parameter in DCE-MRI). Compared with K^{trans}, K_{ep} was affected only by the concentration of contrast agent and the volume fraction in the extracellular space of the tumor vessels and may therefore more accurately reflect the actual permeability of tumor capillaries [17]. This phenomenon indicates that to some extent, the D value is related to the quantitative parameter of DCE-MRI and reflects an opportunity for further research. Only approximately 10% of undifferentiated cancers are considered to be closely related to vascular endothelial growth factor [27, 28]. Further stratification studies correlating histological findings with parameters from IVIM DWI or DCE-MRI may be helpful for clarifying the relationships between IVIM DWI and DCE-MRI of parameters. The AUC of the D value combined with DCE-MRI parameters (K^{trans} and K_{ep}) was significantly powerful, achieving a specificity and PPV of 100%, suggesting the usefulness of IVIM DWI and the quantitative parameters of DCE-MRI in thyroid nodules.

The main limitation of our study was the retrospective design. An analysis of index lesions using retrospectively drawn ROIs manually defined on MRI images by a single reader based on a surgical histology report is subjective and does not assess inter-reader agreement. Second, a relatively small cohort of patients was included in our study design. Therefore, a follow-up investigation is needed to correlate IVIM DWI parameters with various immunohistochemical results.

Conclusion

In conclusion, our results suggest that the perfusion parameters of DCE-MRI in thyroid nodules should not be replaced by those of IVIM DWI. We demonstrated a moderate correlation between the IVIM DWI parameter *D* and the quantitative DCE-MR parameter K_{ep} in the benign group. Therefore, IVIM DWI combined with quantitative DCE-MRI may be a useful imaging tool for the assessment of thyroid nodules in clinical practice.

Disclosure of conflict of interest

None.

Address correspondence to: Dr. Yanfang Jin, Department of MR, Beijing Shijitan Hospital, Capital Medical University, Peking University Ninth School of Clinical Medicine, Tieyilu 10#, Haidian District, Beijing 100038, China. E-mail: sjtjyf@163.com

References

[1] Schob S, Voigt P, Bure L, Meyer HJ, Wickenhauser C, Behrmann C, Hohn A, Kachel P, Dralle H, Hoffmann KT and Surov A. Diffusion-weighted imaging using a readout-segmented, multishot EPI sequence at 3 T distinguishes between morphologically differentiated and undifferentiated subtypes of thyroid carcinoma-a preliminary study. Transl Oncol 2016; 9: 403-410.

[2] Gollub MJ, Gultekin DH, Akin O, Do RK, Fuqua JL, Gonen M, Kuk D, Weiser M, Saltz L, Schrag D, Goodman K, Paty P, Guillem J, Nash GM, Temple L, Shia J and Schwartz LH. Dynamic contrast enhanced-MRI for the detection of pathological complete response to neoadjuvant chemotherapy for locally advanced rectal cancer. Eur Radiol 2012; 22: 821-831.

[3] Khalifa F, Soliman A, El-Baz A, El-Ghar MA, El-Diasty T, Gimel'farb G, Ouseph R and Dwyer AC. Models and methods for analyzing DCE-MRI: a review. Med Phys 2014; 41: 124301.

[4] Nakahara H, Noguchi S, Murakami N, Tamura S, Jinnouchi S, Kodama T, Adjei ON, Nagamachi S, Ohnishi T, Futami S, Flores LG and Watanabe K. Gadolinium-enhanced MR imaging of thyroid and parathyroid masses. Radiology 1997; 202: 765-772.

[5] Yuan Y, Yue XH and Tao XF. The diagnostic value of dynamic contrast-enhanced MRI for thyroid tumors. Eur J Radiol 2012; 81: 3313-3318.

[6] Tunca F, Giles Y, Salmaslioglu A, Poyanli A, Yilmazbayhan D, Terzioglu T and Tezelman S. The preoperative exclusion of thyroid carcinoma in multinodular goiter: dynamic contrast-enhanced magnetic resonance imaging versus ultrasonography-guided fine-needle aspiration biopsy. Surgery 2007; 142: 992-1002; discussion 1002, e1-2.

[7] Tezelman S, Giles Y, Tunca F, Gok K, Poyanli A, Salmaslioglu A and Terzioglu T. Diagnostic value of dynamic contrast medium enhanced magnetic resonance imaging in preoperative detection of thyroid carcinoma. Arch Surg 2007; 142: 1036-1041.

[8] Tofts PS, Brix G, Buckley DL, Evelhoch JL, Henderson E, Knopp MV, Larsson HB, Lee TY, Mayr NA, Parker GJ, Port RE, Taylor J and Weisskoff RM. Estimating kinetic parameters from dynamic contrast-enhanced T(1)-weighted MRI of a diffusable tracer: standardized quantities and symbols. J Magn Reson Imaging 1999; 10: 223-232.

[9] Ben-David E, Sadeghi N, Rezaei MK, Muradyan N, Brown D, Joshi A and Taheri MR. Semiquantitative and quantitative analyses of dynamic contrast-enhanced magnetic resonance imaging of thyroid nodules. J Comput Assist Tomogr 2015; 39: 855-859.

[10] Le Bihan D, Breton E, Lallemand D, Aubin ML, Vignaud J and Laval-Jeantet M. Separation of diffusion and perfusion in intravoxel incoherent motion MR imaging. Radiology 1988; 168: 497-505.

[11] Song MH, Jin YF, Guo JS, Zuo L, Xie H, Shi K and Yue YL. Application of whole-lesion intravoxel incoherent motion analysis using iZOOM DWI to differentiate malignant from benign thyroid nodules. Acta Radiol 2019; 60: 1127-1134.

[12] Tan H, Chen J, Zhao YL, Liu JH, Zhang L, Liu CS and Huang D. Feasibility of intravoxel incoherent motion for differentiating benign and malignant thyroid nodules. Acad Radiol 2019; 26: 147-153.

[13] Jiang J, Xiao Z, Tang Z, Zhong Y and Qiang J. Differentiating between benign and malignant sinonasal lesions using dynamic contrast-enhanced MRI and intravoxel incoherent motion. Eur J Radiol 2018; 98: 7-13.

[14] Zhou N, Chu C, Dou X, Li M, Liu S, Zhu L, Liu B, Guo T, Chen W, He J, Yan J, Zhou Z, Yang X and Liu T. Early evaluation of irradiated parotid glands with intravoxel incoherent motion MR imaging: correlation with dynamic contrast-enhanced MR imaging. BMC Cancer 2016; 16: 865.

[15] Marzi S, Piludu F, Forina C, Sanguineti G, Covello R, Spriano G and Vidiri A. Correlation study between intravoxel incoherent motion MRI and dynamic contrast-enhanced MRI in head and neck squamous cell carcinoma: evaluation in primary tumors and metastatic nodes. Magn Reson Imaging 2017; 37: 1-8.

[16] Xu XQ, Choi YJ, Sung YS, Yoon RG, Jang SW, Park JE, Heo YJ, Baek JH and Lee JH. Intravoxel incoherent motion MR imaging in the head and neck: correlation with dynamic contrast-enhanced MR imaging and diffusion-weighted imaging. Korean J Radiol 2016; 17: 641-649.

[17] Koo HR, Cho N, Song IC, Kim H, Chang JM, Yi A, Yun BL and Moon WK. Correlation of perfusion parameters on dynamic contrast-enhanced MRI with prognostic factors and subtypes of breast cancers. J Magn Reson Imaging 2012; 36: 145-151.

[18] Yeo DM, Oh SN, Jung CK, Lee MA, Oh ST, Rha SE, Jung SE, Byun JY, Gall P and Son Y. Correlation of dynamic contrast-enhanced MRI perfusion parameters with angiogenesis and biologic aggressiveness of rectal cancer: preliminary results. J Magn Reson Imaging 2015; 41: 474-480.

[19] Akslen LA and Livolsi VA. Increased angiogenesis in papillary thyroid carcinoma but lack of prognostic importance. Hum Pathol 2000; 31: 439-442.

[20] Bartolotta TV, Midiri M, Galia M, Runza G, Attard M, Savoia G, Lagalla R and Cardinale AE. Qualitative and quantitative evaluation of solitary thyroid nodules with contrast-enhanced ultrasound: initial results. Eur Radiol 2006; 16: 2234-2241.

[21] Moon HJ, Kwak JY, Kim MJ, Son EJ and Kim EK. Can vascularity at power Doppler US help predict thyroid malignancy? Radiology 2010; 255: 260-269.

[22] Shukla-Dave A, Lee N, Stambuk H, Wang Y, Huang W, Thaler HT, Patel SG, Shah JP and Koutcher JA. Average arterial input function for quantitative dynamic contrast enhanced magnetic resonance imaging of neck nodal metastases. BMC Med Phys 2009; 9: 4.

[23] Shi RY, Yao QY, Zhou QY, Lu Q, Suo ST, Chen J, Zheng WJ, Dai YM, Wu LM and Xu JR. Preliminary study of diffusion kurtosis imaging in thyroid nodules and its histopathologic correlation. Eur Radiol 2017; 27: 4710-4720.

[24] Wu Y, Yue X, Shen W, Du Y, Yuan Y, Tao X and Tang CY. Diagnostic value of diffusion-weighted MR imaging in thyroid disease: application in differentiating benign from malignant disease. BMC Med Imaging 2013; 13: 23.

[25] Hao Y, Pan C, Chen W, Li T, Zhu W and Qi J. Differentiation between malignant and benign thyroid nodules and stratification of papillary thyroid cancer with aggressive histological features: whole-lesion diffusion-weighted imaging histogram analysis. J Magn Reson Imaging 2016; 44: 1546-1555.

[26] Le Bihan D and Turner R. The capillary network: a link between IVIM and classical perfusion. Magn Reson Med 1992; 27: 171-178.

[27] Lam AKY. Pathology of endocrine tumors update: World Health Organization new classification 2017-other thyroid tumors. AJSP Rev Rep 2017; 22: 209-216.

[28] Gule MK, Chen Y, Sano D, Frederick MJ, Zhou G, Zhao M, Milas ZL, Galer CE, Henderson YC, Jasser SA, Schwartz DL, Bankson JA, Myers JN and Lai SY. Targeted therapy of VEGFR2 and EGFR significantly inhibits growth of anaplastic thyroid cancer in an orthotopic murine model. Clin Cancer Res 2011; 17: 2281-2291.